Abstract. This study describes a snowmelt model based on a physical heat balance method. It is an adaptation of the one layer model proposed by Kondo and Yamazaki (1990). As this last one, it takes into account both the heat balance at the snow surface and that of the entire snow cover, and it predicts both the snow surface temperature and the freezing depth. As a new contribution, the model predicts also the evolution of the snow's liquid water content. The energy equation is formulated by means of two energy variables: the Liquid Content and the Cold Content. Percolation depends on mass liquid fraction trough Darcy's law. The model has been validated through field measurements obtained at the instrumented site of Le Col de Porte of the "Centre d'Etudes de la Neige (CEN-Météo France)" corresponding to the winter seasons of 1988/89, 93/94 and 94/95. The results show that the model correctly represents the evolution and melting of the seasonal snow.

1.0. INTRODUCTION

Seasonal snow is not only a significant surface water input of importance to many aspects of hydrology, including water supply, erosion and flood control, but it also influences climate through changes in ground surface properties.

The model was developped initially to predict the rapid snowmelt rates, in order to be coupled with a hydrological model. This one layer model is intended to describe the mass and energy evolution of a snowpack, capturing the essence of its physical processes, with a treatment as simple as possible.

The model combines and adapts the models of Kondo and Yamazaki (1990) and Tarboton et al. (1994) giving simultaneously both the evolution of the freezing depth and the liquid water content.

The paper is divided as follows: Section 2 gives a brief discussion of the physics of the model. In Section 3 the practical method of resolution is exposed. Section 4 describes the data sets that have been used to validate the model and the results of the testing. The conclusions are drawn in Section 5.

2.0. MODEL DESCRIPTION

Remarks:

- From now on, *depth z* means *water equivalent depth z*. 'z' is related to the real depth 'y' by:

$$\rho_w \cdot \delta z = \rho(y) \cdot \delta y \quad (1)$$

where ρ_w and ρ are water and snow densities.

- In the model, snow density is taken into account only to calculate the snowpack depth and the parameterization of the runoff.

2.1. Snowpack structure

The snowpack can be divided into two layers separated by the freezing depth z_o, that is defined as the depth where the snow temperature T reaches the melting point $T_o = 0\ ^0C$ (see Fig. 1). The upper layer is assumed to be dry and with a temperature increasing from the surface temperature T_s to $0\ ^0C$ at freezing depth. The lower layer, which is referred to as the humid layer, has a uniform temperature of $0\ ^0C$ and it can store liquid water. The mass liquid fraction w(z) is the proportion of the total snowpack mass (liquid and solid) that is liquid. w(z) is given in the model

by:

$$w(z) = (0 , \text{if } z<z_o ; w_u , \text{if } z_o \leq z \leq SWE) \quad (2)$$

where w_u is the uniform mass liquid fraction in the humid layer, and SWE is the snow water equivalent.

The liquid water content WC is defined as the thickness of the liquid water inside the snowpack, and it is stored in the humid layer. From (2):

$$WC = w_u \cdot (SWE - z_o) \quad (3)$$

The freezing depth decreases if there is a positive flow of energy and it can eventually disappear.

2.2 Mass balance

The mass balance is represented by the following equation:

$$\frac{\delta SWE}{\delta t} = P_s + P_r + E - M_r \qquad (4)$$

where P_s is snowfall intensity , P_r is rainfall intensity , E is turbulent vapor flux due to latent heat, and M_r is meltwater outflux.

2.3. Energy balance

2.3.1. Liquid, Cold and Energy Contents. The energy quantity Liquid Content LC is related to the liquid water content WC inside the snowpack, which is assumed to be always at 0 ^{0}C. It is defined as the melting heat necessary to obtain the liquid water content from the ice phase

$$LC = WC \cdot \rho_w \cdot L_f \quad (5)$$

where L_f is the heat of fusion of the ice (334400 J kg^{-1}).

The Cold Content CC is related to the temperature change of the snowpack. It is defined as the heat necessary to obtain a uniform temperature of 0 ^{0}C of the reference state from the actual temperature profile of the snowpack.

$$CC = \int_0^H c_s(y)\, \rho_s(y)\, (T_o - T(y))\, dy = \rho_w \int_0^{SWE} c_s(z)\, (T_o - T(z))\, dz \qquad (6)$$

where H is the snowpack depth and c_s is specific heat of the snow.

The Cold Content is approximated in the model as

$$CC(z_o, T_s) = k_{CC} \cdot \rho_w \cdot c_s \cdot z_o \cdot (T_o - T_s) \quad (7)$$

where k_{CC} is a dimensionless calibration parameter referred to as the *Cold content factor*, and c_s is considered constant (2105 J kg^{-1} K^{-1}).

In the model the Cold Content is associated with the dry layer, and the Liquid Content with the humid layer.

The Energy Content U is defined relative to a reference state U_o of water at 0 ^{0}C in the ice phase. Variations of the Energy Content result in changes of the liquid water content or/and changes in temperature. From the former definitions of Liquid and Cold Contents the Energy Content is then defined as:

$$U = LC - CC \quad (8)$$

2.3.2. Energy processes. The Contents described above can change due to rainfall, percolation, as well as due to the heat balance flow Q of the entire snowpack (Q includes all the heat transfers to and from the snowpack: see the Appendix A).

Rainfall and percolation change the liquid water content and the related Liquid Content. In analogy with Eq. (5),

$$Q_{rm} = P_r \cdot \rho_w \cdot L_f \quad (9)$$

$$Q_m = - M_r \cdot \rho_w \cdot L_f \quad (10)$$

are the energy flows related to rainfall and percolation respectively.

Change in Contents produced by the heat balance flow Q of the entire snowpack depends on Q's sign:

- If Q is positive the Cold Content decreases and melting is produced once CC reaches a 0 value.
- If Q is negative the Cold Content increases. When it is less than SWE, the freezing depth also increases, and if there is liquid water content internal refreezing is produced.

The energy balance is then given by the equation:

$$\frac{\delta U}{\delta t} = Q_{rm} + Q_m + Q \quad (11)$$

2.3. Percolation scheme.

The percolation scheme is considered as an independent process and it is an adaptation from Tarboton et al. (1994):

Darcy's law for flow through porous media is used to determine the outflow rate M_r

$$M_r = k_{sat} \cdot s^{*3} \quad (12)$$

where k_{sat} is the snow saturated hydraulic conductivity, used in the model as a second calibration parameter, and s* is the relative saturation in excess of water retained by capillary forces. s* is given by

$$s^* = \frac{w_u - w_o}{\frac{\rho_w}{\rho} - \rho_{wover}\,\rho_i - w_o} \quad (13)$$

where w_o is the retention capacity (see Appendix A), ρ is the mean snow density and ρ_i is the ice density (917 kg m^{-3})

3.0. PRACTICAL RESOLUTION

The different physical processes affecting the snowpack evolution are solved as follows:

If Q_o is the heat flow at the snow surface (see Appendix A), and Q and Q_o are considered as depending only on snow surface temperature, then the *equilibrium surface temperatures* T_{se} and T_{seo} are respectively defined through the equations: $Q(T_{se}) = 0$ and $Q(T_{seo}) = 0$.

Internal melting and evolution of the surface temperature and freezing depth at a time interval $\Delta t = t(2) - t(1)$, are obtained through the following algorithm (Fig. 2):

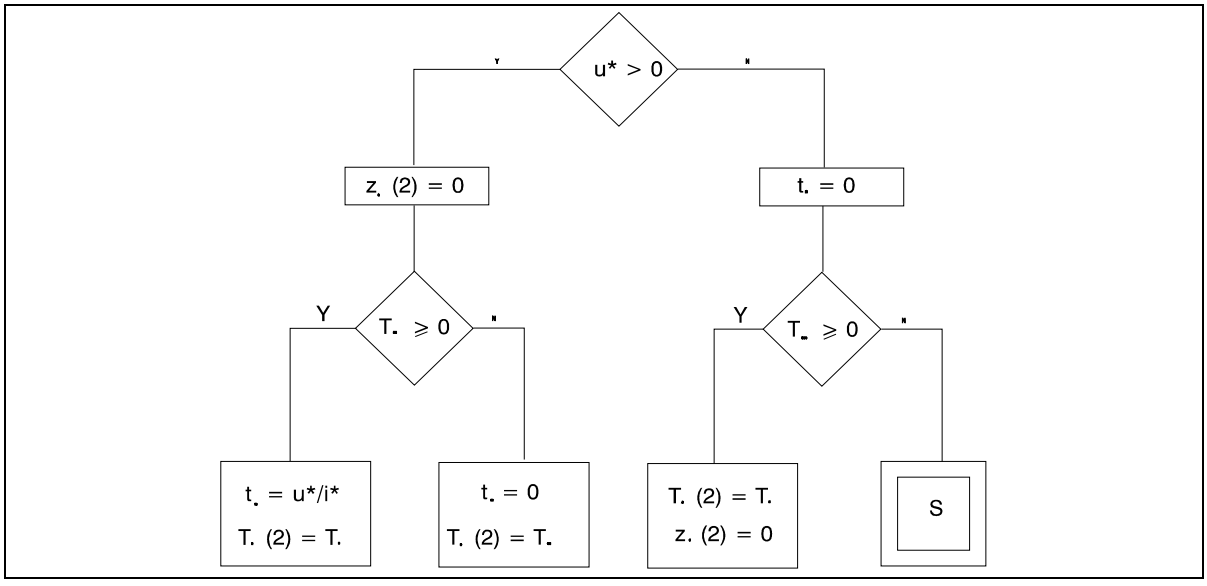

- Fig. 2 -

where

$i^* = (Q(T_s(1))+Q(T_o))/2$

$u^* = - CC(1) + i^* \cdot \Delta t = - k_{CC} \cdot \rho_w \cdot c_s \cdot z_o \cdot (T_o - T_s(1)) + i^* \cdot \Delta t$

and t_m is the melting period

$T_s(2)$ and $z_o(2)$ in the S case are the meaningful solutions of the system:

$$U(2) = U(1) + \langle Q \rangle \cdot \Delta t \quad (14)$$

$$Q_o(T_s(2)) + k_\lambda \cdot (T_o - T_s(2))/z_o(2) = 0 \quad (15)$$

<Q> , in Eq. (14), is the mean value of Q in the time interval, and Eq. (15) is an adaptation of the equation of heat conduction at the snow surface, where $Q_o(T_s)$ is the heat flow at the snow surface and k_λ is the *equivalent thermal conductivity of the snow* used in the model as a third calibration parameter. To solve this system, $Q_o(T_s)$ and $Q(T_s)$ are previously linearized in T_s.

The algorithm finishes updating the liquid water content when there is melting ($t_m>0$)

$$\Delta WC = t_m \cdot Q(T_o)/(L_f \cdot \rho_w) \quad (16)$$

or when there is internal refreezing ($z_o(2) > z_o(1)$)

$$\Delta WC = -w_u \cdot (z_o(2)-z_o(1)) \quad (17)$$

Changes of mass and liquid water content due to precipitation, surface water vapor flux and percolation, are calculated separately.

Depth is obtained through the snow water equivalent and the parameterized snow density.

Appendix A gives brief descriptions of how the different heat flows are obtained, as well as the parameterizations of albedo, snow density and retention capacity.

4.0. TESTING AND RESULTS

4.1. Description of the data set

The model's calibration and validation have been made through field measurements obtained at the instrumented site of Le Col de Porte that belongs to the 'Centre d'Etudes de la Neige' of Météo-France. This center is located at an altitude of 1320 m. in the French Northern Alps.

Continuous snow cover usually lies from late November to the begining of May. Deep snow is wet most of the time, but the snow's upper layer is exposed to varied conditions depending on the weather. The soil is covered with short grass, so the vegetation has no impact on the snow's evolution.

The version of the model that has been tested needs the following input data: snow and rain precipitations, atmospheric pressure, air temperature and humidity, wind speed, solar and infrared incoming radiation, and albedo. All these inputs to the model, except the pressure, are measured at the laboratory. The albedo is measured daily, and the rest of the variables are measured hourly. The pressure is taken as a constant from the Standard Atmosphere: 863 hPa.

The model is run with a time step of one hour and its main outputs are: snow depth, water equivalent, surface temperature, freezing depth, liquid water content and runoff. The depth and surface temperature are measured hourly and the runoff daily at Le Col de Porte.

The model has been tested for three winters: 88/89, 93/94 and 94/95. The albedo was not measured during the winter 93/94 and was parameterized in this season. The model was also run with the parameterized albedo for the other two seasons. The periods of testing for the three winters are: 17/12/1988 - 08/05/1989; 10/11/1993 - 10/05/1994; and 17/12/1994 - 20/05/1995.

4.2. Results

The values of the three calibration parameters, the Cold Content factor k_{cc} , the *equivalent thermal conductivity of the snow* k_{λ} , and the snow saturated hydraulic conductivity k_{sat} , were obtained comparing graphically and numerically the measures of the snow depth, surface temperature and runoff, with the simulated values for the season 88/89. The selected values were applied to the other two seasons and are:

$$k_{cc}= 0.1;\ k_{\lambda} = 0.26\ \text{W m}^{-1}\ \text{K}^{-1};\ \text{and}\ k_{sat} = 8\cdot10^{-4}\ \text{m s}^{-1}.$$

Results of these comparisons show, in general, a good agreement between measured and simulated snow depth, surface temperature and runoff. The graphical comparisons are shown in the Figures 3-14, and numerical comparisons are given in Tables 1-3.

Simulations of the snow depth (Fig. 4,9,12) show that when the albedo is measured, the simulated ablation periods are slightly (88/89) or significally (94/95) shorter than the measured ones. When the albedo is parameterized, the simulated period matches (93/94, 94/95) or exceeds (88/89) the measured ones. In the case of the measured albedo, a possible cause of this fact may come from its slight underestimation, especially during the melting period, due to the snow melting which takes place at the foot of the instrumented pylon and is caused by the albedometer itself.

The parameterized albedo (Fig. 3, 9, 12) performs well in simulating the observed fluctuations. The main discrepancy consist in a weaker decay compared with that of the measured albedo, and in many cases this accounts for the slight overestimation of the parameterized albedo .

Fig. 8 shows a good general agreement between simulated and observed surface temperatures for three different periods of the 88/89 season. Changes of thermal conductivity (e.g. after a snowfall), or lack of parameterization for the soil interaction, may be some of the reasons for the discrepancies.

Fig. 5, 11, 14 compare measured and simulated daily bottom water runoff. The slight underestimation of the measured albedo in strong melting periods, and its related shortening of the ablation period, help to explain the better general performance of the simulated runoff when the albedo is parameterized.

Fig. 6, 7 simulate the snow water equivalent, the humid layer depth, the liquid water content, the mass liquid fraction in the humid layer and the retention capacity for the 88/89

season when the model is run with the measured albedo.

Tables 1-3 collect some overall numerical comparisons between measured and simulated surface temperatures, snow depth and runoff, for the three seasons.

5.0. CONCLUSIONS

The model captures the main physical processes of the snow's evolution including the internal refreezing of the liquid water content. It predicts accurately enough runoff, depth and surface temperature, while remaining a simple one layer energy balance model.

Two final remarks about the applicability of the model:

- the model has only been tested with data from Le Col de Porte. It remains to be tested wether the adjusted calibration parameters k_{CC} , k_{λ} and k_{sat} are valid elsewhere or they should be tuned for the model application at a different location.
- The model is a point model. A distributed model that takes into account orography and vegetation, among other factors, is needed if it is to be applied to a vast region.

APPENDIX A

HEAT FLOWS AND SNOW DENSITY, ALBEDO AND RETENTION CAPACITY PARAMETERIZATIONS

Heat surface flow Q_o is calculated as

$$Q_o = Q_{li} - Q_{le} + Q_h + Q_e + Q_s \quad (A.1)$$

and heat balance flow of the entire snowpack Q as:

$$Q = Q_o + Q_{sn} + Q_{rt} \quad (A.2)$$

where Q_{li} is the incoming longwave radiation; Q_{le} the outgoing longwave radiation; Q_h , the sensible heat flux; Q_e the latent heat flux,; Q_s the advected heat from snow precipitation; Q_{sn} the net shortwave radiation; and Q_{rt} the advected heat from rain, respectively.

Radiation. Incoming longwave radiation Q_{li} is directly measured. Net shortwave radiation Q_{sn} is given by:

$$Q_{sn} = Q_{si} \cdot (1-\alpha_s) \quad (A.3)$$

where Q_{si} is the incoming shortwave radiation that is directly measured, and α_s is the snow albedo.

The outgoing longwave radiation is

$$Q_{le} = \varepsilon_s \cdot \sigma \cdot T_s^4 \quad (A.4)$$

where $\varepsilon_s = 1$ is the snow emissivity, σ the Stephan-Boltzman constant (5.67×10^{-2} W m^{-2} K^{-4}) and T_s is the absolute snow surface temperature.

Turbulent fluxes, Q_h and Q_e. Sensible and latent fluxes between the snow surface and air above are modeled using the concept of flux proportional to temperature and vapor pressure gradients

with constants of proportionality, the so-called turbulent transfer coefficients.

Q_h is given by:

$$Q_h = c_h \cdot v \cdot \rho_a \cdot c_p \cdot (T_a - T_s) \quad (A.5)$$

where c_h is an adimensional coefficient (0.023), v the 10 m wind speed (ms^{-1}), ρ_a the air density (determined from the atmospheric pressure and air the temperature T_a), c_p the air specific heat capacity (1005 J kg^{-1} K^{-1}), and T_s the snow surface temperature.

Surface vapor transport flux M_e is given by:

$$M_e = c_e \cdot v \cdot (e_a - e_s(T_s))/(R_v \cdot T_a) \quad (A.6)$$

where c_e is an adimensional coefficient (0.023), $e_a - e_s(T_s)$ the difference in vapor pressure between the air and the snow surface, and R_v is the water vapor constant (461 J kg^{-1} K^{-1}).

Latent flow Q_e is:

$$Q_e = L_{s/v} \cdot M_e \quad (A.7)$$

where $L_{s/v}$ is the latent heat of sublimation ($2.834 \cdot 10^6$ J kg^{-1}) for cold snow, or evaporation ($2.5 \cdot 10^6$ J kg^{-1}) for wet snow.

The water equivalent depth flux E due to latent heat is calculated as:

$$E = M_e / \rho_w \quad (A.8)$$

where ρ_w is the water density.

Advected heat from precipitation Q_{rt} , Q_s. The advected heat from rain Q_{rt} is:

$$Q_{rt} = P_r \cdot \rho_w \cdot c_w \cdot (T_r - T_o) \quad (A.9)$$

where P_r is the rain intensity (m s^{-1}), c_w the specific heat of water (4186 J kg^{-1} K^{-1}), and T_r the rain temperature parameterized as: $T_r = \max(T_a, T_o)$, with T_a being the air temperature.

The advected heat from snow precipitation Q_s is:

$$Q_s = P_s \cdot \rho_w \cdot c_S \cdot (T_{sn} - T_o) \quad (A.8)$$

where P_s is the snowfall intensity, c_s the specific heat of snow (2105 J kg^{-1} K^{-1}), and T_{sn} is the snow precipitation temperature parameterized as: $T_{sn} = \min(T_a, T_o)$

Snow density. Snow density ρ is calculated with an adaptation of the Loth et al. (1993) parameterization. ρ is considered uniform, and its evolution is given by:

$$(\partial\rho(t)/\partial t)/\rho(t) = a \cdot \exp(- b \cdot (T_o - T_s /2 - c(\rho(t) - \rho_d)) \quad (A.9)$$

with $a = 2.8 \cdot 10^{-6}$ s^{-1}, $b = 4 \cdot 10^{-2}$ K^{-1}, $c = (0.0$ if $\rho \leq \rho_d$, $4.6 \cdot 10^2$ if $\rho > \rho_d$; $\rho_d = 250$ kg $m^{-3})$

When there is snowfall, ρ is recalculated as the weighted average of the previous density and that of the recent new snow $\rho_n = 100$ kg m^{-3}.

If P_r is rain intensity, ρ is recalculated with the empirical formula:

$$(\partial\rho/\partial t)/\rho = k_r \cdot (P_r/SWE) \quad (A.10)$$

with $k_r = 2$, and where SWE is the snow water equivalent.

Retention capacity. The parameterization of Loth et al. (1993) is adopted:

The porous structure of snow and molecular interactions between water and ice particles enables a snow mass to store liquid water up to a threshold value w_o of its mass liquid fraction w_u . w_o is defined as the retention capacity and is given by:

$$w_o = (w_{min} \text{ , if } \rho \geq \rho_e \text{ ; } w_{min} + (w_{max}-w_{min}) \cdot (\rho_e-\rho)/\rho_e \text{ , if } \rho < \rho_e) \quad \text{(A.11)}$$

with $w_{min} = 0.03$, $w_{max} = 0.1$, $\rho_e = 200$ kg m^{-3}.

Albedo. The albedo α_s is calculated following Douville et al. (1995):

$$\alpha_s(t+\Delta t) = \alpha_s(t) - \tau_a \cdot \Delta t/\tau_1 \text{ , if } T_s < T_o$$

$$\alpha_s(t+\Delta t) = (\alpha_s(t)-\alpha_{min}) \exp(- \tau_f \cdot \Delta t/\tau_1) + \alpha_{min} \text{ , if } T_s = T_o$$

(A.12)

with $\tau_1 = 86400$ s, $\tau_a = 0.008$, $\tau_f = 0.24$ and $\alpha_{min} = 0.5$. A snowfall refreshes the albedo back to 0.85 when it exceeds the threshold value of 10 mm.

APPENDIX B

ACCUMULATED MASS AND LIQUID WATER CONTENT BALANCES

The integration of the mass balance equation (Eq. 4) in a period $\Delta t = t(2)- t(1)$ gives:

$$SWE(2) = SWE(1) + S + R + E_T - M_T \quad \text{(B1)}$$

where SWE(1) and SWE(2) are the initial and final snow water equivalent; S the accumulated snowfall; R the accumulated rainfall; E_T the accumulated sublimation; and M_T the accumulated runoff.

In the same way, the integration of the liquid water content balance gives:

$$WC(2) = WC(1) + R + IM - IR - M_T \quad (B2)$$

where IM is the accumulated internal melting; and IR is the accumulated internal refreezing.

Table B1 collects the different terms of these balances for the measurement periods of the three seasons. SWE(1) and WC(1) are initially zero, except for the estimations made for the season 88/89. S and R are directly measured, and the rest of the variables are obtained from the simulations. From this table we see the importance of the internal refreezing in the snow evolution. The comparison of the IR/IM and S/(S+R) ratios characterize the season 88/89 as the coldest of the three seasons.

APPENDIX C: LIST OF SYMBOLS AND UNITS

α_s snow albedo.

ε_s snow emissivity.

ρ snow density, kg m^{-3}.

ρ_a air density, kg m^{-3}.

ρ_i ice density, kg m^{-3}.

ρ_w water density, kg m^{-3}.

σ Stephan Boltzman constant, W m^{-2} K^{-4}.

CC Cold Content, J m^{-2}.

c_p air specific heat capacity, J kg^{-1} k^{-1}.

c_s snow specific heat , J kg^{-1} K^{-1}.

c_w water specific heat capacity, J kg^{-1} k^{-1}.

E water equivalent depth flux due to latent heat, m s^{-1}.

e_a vapor pressure in the atmosphere, Pa.

e_s vapor pressure within the snow, Pa.

E_T water equivalent accumulated depth due to latent heat, m.

H snowpack depth, m.

IM accumulated internal melting, m.

IR accumulated internal refreezing, m.

k_λ equivalent thermal conductivity of the snow, W m^{-1} K^{-1}.

k_{CC} Cold Content factor.

k_{sat} snow saturated hydraulic conductivity, m s^{-1}.

LC Liquid Content, J m^{-2}.

L_f latent heat of fusion of the ice, J kg^{-1}.

L_s latent heat of sublimation of the ice, J kg^{-1}.

L_v latent heat of evaporation of the ice, J kg^{-1}.

M_e water vapor flux due to latent heat, kg m^{-2} s^{-1}.

M_r runoff, m s^{-1}.

M_T accumulated runoff, m.

P_r rainfall intensity, m s^{-1}.

P_s snowfall intensity, m s^{-1}.

Q heat balance flow of the entire snowpack, W m^{-2}.

Q_e latent heat flux, W m^{-2}.

Q_h sensible heat flux, W m^{-2}.

Q_{le} outgoing longwave radiation, W m^{-2}.

Q_{li} incoming longwave radiation, W m^{-2}.

Q_m energy flow related to percolation, W m^{-2}.

Q_o heat surface flow, W m^{-2}.

Q_{rm} energy flow related to rain, W m^{-2}.

Q_{rt} advected heat from rain, W m^{-2}.

Q_s advected heat from snow precipitation, W m^{-2}.

Q_{si} incoming shortwave radiation, W m^{-2}.

Q_{sn} net shortwave radiation, W m^{-2}.

R accumulated rainfall, m.

R_v water vapor constant, J kg^{-1} k^{-1}.

S accumulated snowfall, m.

SWE snow water equivalent, m.

s^* relative saturation.

T snow temperature, K.

T_a 2m air temperature, K.

t_m melting period, s.

T_o ice melting point, K.

T_r rain temperature, K.

T_s snow surface temperature, K.

T_{se} equilibrium surface temperature related to Q, K.

T_{seo} equilibrium surface temperature related to Q_o, K.

T_{sn} snow precipitation temperature, K.

U Energy content, J m^{-2}.

U_o Energy content reference state, J m^{-2}.

v 10m wind velocity, m s^{-1}.

w mass liquid fraction.

WC liquid water content, m.

w_o retention capacity.

w_u uniform mass liquid fraction in the humid layer.

y depth, m.

z water equivalent depth, m.

z_o water equivalent freezing depth, m.

Acknowledgements. I am grateful to Eric Brun, Yves Durand and Eric Martin, of the 'Centre d'Etudes de la Neige', for their generous attitude concerning my access to the data, which made possible the development and validation of this model.

References

- Douville H et al. (1995). A new snow parameterization for the Météo-France climate model. Climate Dynamics 12:21-35.

- Kondo J, Yamazaki T (1990). A prediction model for snowmelt, snow surface temperature and freezing depth using a heat balance method. J Appl Meteorol, 29:375-384.

- Loth B et al. (1993). Snow cover model for global climate simulations. J Geophys Res, 98:10451-10464.

- Tarboton DG et al. (1994). A spatially distributed energy balance snowmelt model. Working Paper WP-94-HWR-DGT/003. Utah Water Research Laboratory, Utah State University.

winter	N	r	M	SD	PAD
88/89	3380	0.83	-2.9	12.0	21
88/89 *	3380	0.52	7.2	20.2	36
93/94 *	4369	0.93	11.4	21.5	29
94/95	3697	0.96	-5.6	19.9	17
94/95 *	3721	0.97	8.9	20.9	20

- Table 1. **SNOWPACK DEPTH (cm) -**

winter	N	r	M	SD	PAD
88/89	2870	0.97	0.2	1.0	19
88/89 *	2881	0.97	0.2	1.1	21
93/94 *	4369	0.94	0.4	1.4	26
94/95	3696	0.94	0.3	1.5	30
94/95 *	3698	0.93	0.2	1.6	32

- Table 2. **SURFACE TEMPERATURE (^{0}C) -**

winter	N	r	M	SD	PAD
88/89	141	0.75	-0.7	6.2	44
88/89 *	141	0.94	-1.1	3.1	35
93/94	31	0.96	2.8	5.3	47
94/95 (lis. 5m^2)	153	0.71	-0.4	9.0	55
94/95 (lis. 1m^2)		0.76	-0.9	8.3	43
94/95 * (lis. 5m^2)	154	0.90	-0.5	5.3	20
94/95 * (lis. 1m^2)		0.88	-0.9	5.9	37

- Table 3. **RUNOFF (mm) -**

Tables 1-3. Numerical comparison between observed and simulated snow depth (Table 1), snow surface temperature (Table 2) and runoff (Table 3) at Le Col de Porte during the winters of 88/89, 93/94, 94/95. Simulations are run with the albedo measured or parameterized (*).Two different observations where made for the runoff of the season 94/95 corresponding to lysimeters of 1m^2 or 5m^2 . N: number of comparison pairs, r: correlation coefficient, M: mean of the differences, SD: standard deviation of the differences, and PAD: percentage of area differences, defined as:

winter	days	SWE(1)	WC(1)	S	R	E_T	IM	IR	M_T	SWE(2)	WC(2)
88/89				474		0	815	278	615	0	0
88/89*	141	63	0	4	77	0	804	296	584	31	2
93/94*	182	0	0	767	366	12	1082	304	1145	0	0
94/95						10	1107	317	1317	0	0
94/95*	154	0	0	780	527	10	1109	319	1318	0	0

$PAD = 100 \frac{\sum_{i=1}^{N} /simulated\ value(i) - measured\ value(i)/}{\sum_{i=1}^{N} /measured\ value(i)/}$

Table B1. Mass and water accumulated components at Le Col de Porte during the seasons of 88/89, 93/94 and 94/95. The model is run with the albedo measured or parameterized (*). The components (mm.) are: SWE(1) and SWE(2) the initial and final snow water equivalent, WC(1) and WC(2) the initial and final liquid water content, S the accumulated snowfall, R the accumulated rainfall, E_T the accumulated sublimation, IM the accumulated melting, IR the accumulated internal refreezing and M_T the accumulated meltwater outflow.

FIGURE CAPTIONS

Fig. 1. Snowpack structure: Schematic snow temperature and mass liquid fraction profiles.

Fig. 2. Algorithm to obtain internal melting as well as evolution of surface temperature and freezing depth at a time interval.

Fig. 3-5. Comparison between observed and simulated hourly snow depth (Fig. 4) and daily runoff (Fig. 5) at Le Col de Porte during the winter of 88/89. There are two simulations: one where the albedo is measured daily and the other where the albedo is parameterized hourly (Fig. 3).

Fig. 6-7. Hourly simulated snow water equivalent, humid layer equivalent depth and liquid water content (Fig. 6), as well as mass liquid fraction and retention capacity (Fig. 7) at Le Col de Porte during the winter of 88/89.

Fig. 8. Comparison between hourly observed and simulated snow surface temperature at Le Col de Porte during different periods of the winter of 88/89.

Fig. 9-11. Comparison between observed and simulated hourly snow depth (Fig. 10) and daily runoff (Fig. 11) at Le Col de Porte during the winter of 93/94. The albedo is parameterized hourly (Fig. 9).

Fig. 12-14. Comparison between observed and simulated hourly snow depth (Fig. 13) and daily runoff (Fig. 14) at Le Col de Porte during the winter of 93/94. There are two simulations: one where the albedo is measured daily and the other where the albedo is parameterized hourly (Fig. 12).